Progress In Electromagnetics Research Letters, Vol. 61, 71–76, 2016

Dual Broadband Metamaterial Polarization Converter in Microwave Regime

Dong Yang[1], Hai Lin[1, *], and Xiaojun Huang[1, 2]

Abstract—Polarization converters based on metamaterial have broad application in imaging, sensing and communication from microwave to optical frequency. However, its performance is limited by single function and narrowband. In this paper, a new type of polarization converter based on square loop shaped metamaterial has been presented. It works in the reflection mode to achieve broadband polarization conversion for both circular and x/y linear polarization waves. The incident linearly polarized wave will be converted to its cross-polarized state with a polarization conversion ratio (PCR) lager than 0.9 in two distinct broad frequency ranges; on the other hand, circularly polarized wave will be reflected to its co-polarized state efficiently in the same spectrum regimes. Good agreements have been observed for both simulation and measurement results. This work offers a further step in developing high performance multi-function microwave or optical devices.

1. INTRODUCTION

Metamaterial (MM), first known as a left-handed material proposed by Veselago in 1968 [1], has exhibited unique EM properties unavailable in nature, such as negative refraction [2, 3], invisible cloaking [4, 5], biosensing [6, 7]. Except these novel applications, MMs have recently been proposed to manipulate polarization states of EM waves [8–11]. Polarization is an ever present issue for achieving full control over electromagnetic (EM) wave propagation [12]. Polarization state can not only represent an intrinsic feature of EM waves, but also offer an extra degree of freedom to manipulate EM waves for various applications. In order to realize such control, it is necessary to create devices that allow 0 to 2π phase modulation and/or devices that allow controlling the amplitude of EM waves [13]. Conventional polarization conversion is realized using optical gratings and birefringent materials such as crystalline solids and liquid crystals [14, 15]. The propagation length in these traditional materials is much larger than the wavelength, which results in a bulky volume, thus it prevents the converter from being integrated into micro-optical systems. Recently, many anisotropic or chiral MM-based structures have been applied to manipulate polarizations of EM waves from microwave to optical frequency regimes [16–20]. Single function linear or circular polarizers have also been demonstrated by using well designed metamaterial unit cells [21–24]. However, to meet the requirement of practical potential applications, the currently available designs should have multiple-function, broad bandwidth and easily fabricated unit cell geometry.

In this paper, a dual-broadband linear polarization conversion using planar MM consisting of very simple inclined metal rectangle loop arrays is presented. The linearly polarized wave can be reflected to its cross-polarized wave when EM wave is normally incident to the designed MM; meanwhile, the reflect wave of circularly polarized incidence will maintain its polarization state due to the unique symmetric design. High polarization conversion ratio larger than 0.9 is obtained for both linear and

Received 30 March 2016, Accepted 17 June 2016, Scheduled 14 July 2016

* Corresponding author: Hai Lin (linhai@mail.ccnu.edu.cn).

[1] College of Physical Science and Technology, Central China Normal University, Wuhan 430079, China. [2] College of Physics and Electrical Engineering, Kashgar University, Kashgar 844000, China.

circular polarizations in the two independent frequency bands. The proposed MM has an uncomplicated geometry but wide bandwidths compared with previous designs [25–28], and can be used in applications such as antenna radome, remote sensors and radiometer.

2. SIMULATION AND EXPERIMENT

Figure 1 depicts the perspective view of the unit cell structure and part of a photograph of the measured sample. The unit cell is composed of a simple inclined metallic rectangular loop on the top of an FR4 substrate which is grounded by copper layers. Dielectric constant of the FR4 substrate is 4.4, its dielectric loss tangent 0.025, and the thickness of the substrate 3.0 mm. The electric conductivity of the copper grounding layer is set to $\sigma = 5.8 \times 10^7$ S/m. The dimensions of the MM unit have been optimized to ensure that the MM-based polarizer can have a wide working frequency band. The optimized geometric parameters of the unit cell are: $p = 11$ mm, $L = 10$ mm, $W = 3.1$ mm, $G = 0.9$ mm, $H = 7.8$ mm.

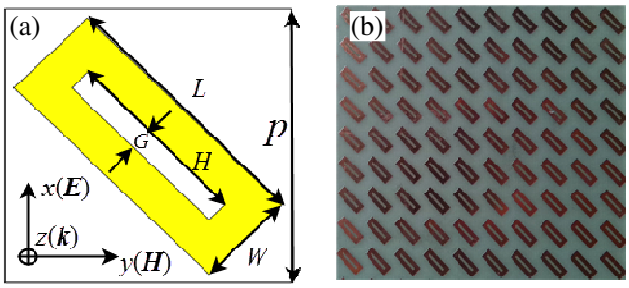

Figure 1. (a) Perspective views of the unit cell structure, (b) part of a photograph of the measured sample.

The simulations were accomplished via the commercial software CST Microwave Studio, which utilizes a finite integration technique and Floquet mode analysis to resolve the frequency response of periodical structure. In simulations, the unit cell boundary conditions were applied in the x and y directions, and open boundary conditions were used in the z direction. Experiments have also been done to test the polarization rotation behavior of the fabricated sample. Without loss of generality, the fabricated sample of the polarization convertor consists of 20×20 unit cells which is stamped on a printed circuit board (PCB). A vector network analyzer (Agilent E8362B) and a pair of stand gain broadband horn antennas are used to measure the reflection coefficient from the sample in an anechoic chamber. Two horns are connected to the vector network analyzer via cables, and the designed MMs are placed in front of the horns. To measure the polarization conversion performance for linear incidence wave, horn 1 is fixed with horizontal polarization in order to emit x-polarized incident waves which will be reflected by the MM, and horn 2 is placed with vertical polarization and horizontal polarization to obtain reflective coefficients $\mathbf{r}_{xx}$ and $\mathbf{r}_{yx}$, respectively. The reflection coefficients for CP wave can be measured in a similar manner. In order to obtain more accurate measurement result, the reflection from a metal plate without the polarizer is used for normalization.

3. RESULTS AND DISCUSSION

Because of the symmetry of the structure along x and y axes, the complex co- and cross-polarized reflective coefficients will not change when the incident wave is x- or y-polarized. Thus, Fig. 2 only shows the simulated and experimental results for an incident x-polarized wave. The transmission of the proposed MM is zero because the copper layer is introduced beneath the structure. $\mathbf{r}_{ij}$ refers to the complex amplitude (linear amplitude) of the i-polarized component of the reflected wave when a j-polarized wave incidence with unit power, where the subscripts i and j can be x or y. Fig. 2(a) shows the simulated and experimental linear polarization reflection spectra of cross-polarization $|\mathbf{r}_{yx}|$ and co-polarization $|\mathbf{r}_{xx}|$ in the frequency range of 4–17 GHz. From Fig. 2(a), the simulated cross-polarization

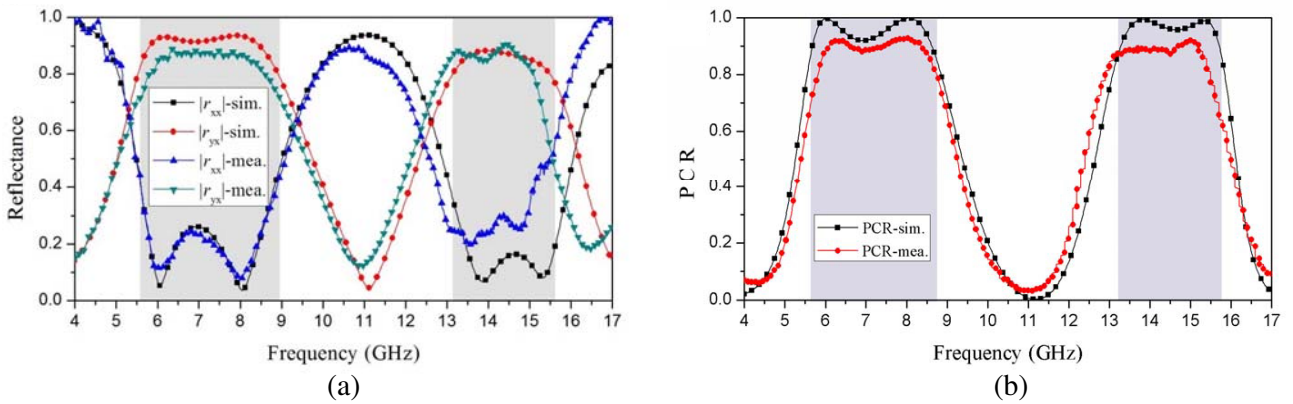

Figure 2. Simulated and experimental results of linearly polarized waves, (a) reflection spectra of co-polarization and cross-polarization, (b) polarization conversion ratio.

reflectance $|\mathbf{r}_{yx}|$ over 0.8 emerges in 5.50–8.94 GHz and 13.10–15.50 GHz; meanwhile, the co-polarization reflectance $|\mathbf{r}_{xx}|$ is less than 0.30 in the same frequency range. Accordingly, the bandwidths of cross-polarization conversion for the incident wave are of 47.75% and 16.78% of the central wavelength, respectively. It means that x-polarized EM wave is converted to y-polarization after being reflected from the MM within the operational frequency range. The experimental spectrum is in good agreement with the simulation, which confirms the results of the simulation. We use polarization conversion ratio (PCR) to describe the performance of frequency-dependent polarization conversion for linear EM waves. The PCR of x- and y-polarized incident waves can be defined as

$$\mathrm{PCR}_x = |\mathbf{r}_{yx}|^2 \Big/ \left(|\mathbf{r}_{yx}|^2 + |\mathbf{r}_{xx}|^2\right) \tag{1a}$$

$$\mathrm{PCR}_y = |\mathbf{r}_{xy}|^2 \Big/ \left(|\mathbf{r}_{xy}|^2 + |\mathbf{r}_{yy}|^2\right) \tag{1b}$$

Figure 2(b) illustrates the simulated and experimental results of PCR for x-polarized incident wave in the frequency range of 4–17 GHz. Apparently, the simulated result of PCR is larger than 0.90 in the frequency ranges of 5.70–8.62 GHz and 13.30–15.50 GHz.

In the same way, the circularly polarized wave conversion can be defined as follows:

$$\mathrm{PCR}_+ = |\mathbf{r}_{++}|^2 \Big/ \left(|\mathbf{r}_{++}|^2 + |\mathbf{r}_{-+}|^2\right) \tag{2a}$$

$$\mathrm{PCR}_- = |\mathbf{r}_{--}|^2 \Big/ \left(|\mathbf{r}_{--}|^2 + |\mathbf{r}_{+-}|^2\right) \tag{2b}$$

The simulated and experimental results for circular polarization is portrayed in Fig. 3. From Fig. 3(a), we notice that the simulated co-polarization reflectance $|\mathbf{r}_{++}|$ is larger than 0.8, while the cross-polarization reflectance $|\mathbf{r}_{-+}|$ is less than 0.30 at the frequency ranges of 5.50–8.94 GHz and 13.10–15.50 GHz. The simulated and experimental results of PCR are also illustrated in Fig. 3(b). PCR of circular polarization is larger than 0.9 in the frequency ranges of 5.70–8.62 GHz and 13.30–15.70 GHz. Compared to the numerical and experimental results, slight frequency discrepancies occur. We attribute such minor differences to fabrication tolerance as well as the dielectric board material whose actual dielectric constant is slightly different from the value used in the simulations. In the experiment, the angle between emitting and receiving antennas is about 5°, while the condition of vertical incidence is used in the simulations, which cannot be neglected.

The polarization conversion efficiency here is ascribed to the superposition of the partial cross-polarized (co-polarized) reflected fields within the Fabry-Perot-like cavity formed by the bottom copper plane and the topmost rectangular structure array, resulting in constructive (destructive) interference and nearly unity (zero) cross-polarized (co-polarized) reflection [26, 29]. In addition, to

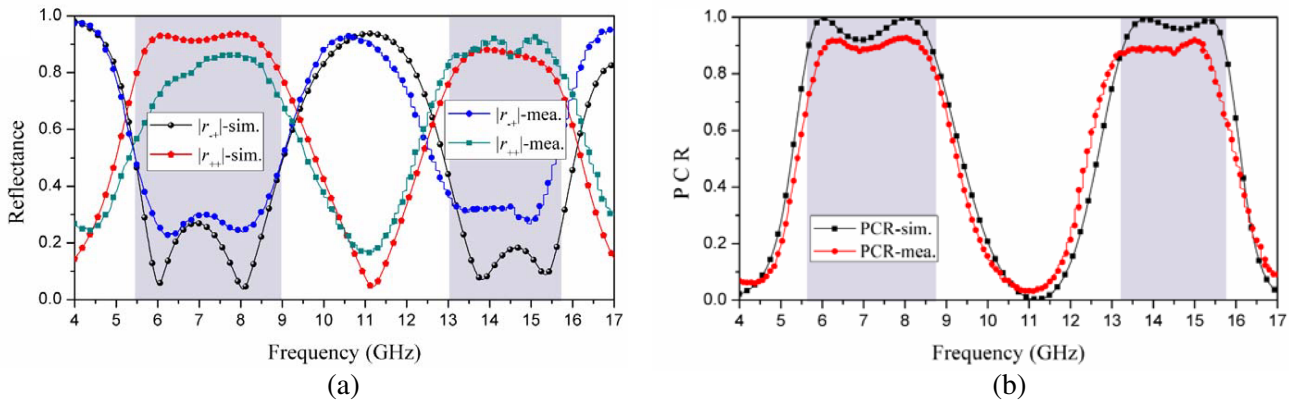

Figure 3. Simulated and experimental circularly polarized waves, (a) reflection spectra of co-polarization and cross-polarization, (b) polarization conversion ratio.

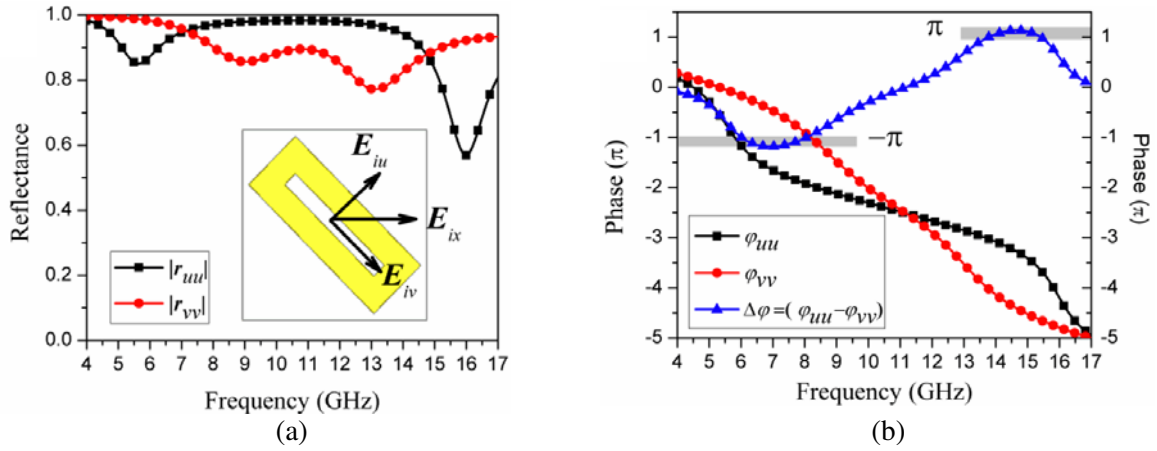

Figure 4. (a) Reflectance and (b) phase for the incident EM polarized along the u and v axes.

better understand the physical mechanism of linear polarization conversion, we take the x-polarized incident EM wave ($\mathbf{E}_{ix}$) as an example and decompose it into two perpendicular components ($\mathbf{E}_{iu}$ and $\mathbf{E}_{iv}$) to study the corresponding reflection response [30], shown in Fig. 4(a). Consider the normal incidence for simplicity, suppose that the incident and reflected waves are given by [26]:

$$\mathbf{E}_{ix} = E_u e^{i(-kz-\omega t)}\hat{u} + E_v e^{i(-kz-\omega t)}\hat{v} \tag{3a}$$

$$\mathbf{E}_{rx} = E_u e^{i(kz-\omega t+\varphi_{uu})}\hat{u} + E_v e^{i(kz-\omega t+\varphi_{vv})}\hat{v} \tag{3b}$$

and the phase difference of the reflection for the incident wave polarized along the u- and v-axes can be described by $\Delta\varphi_{uv} = \varphi_{uu} - \varphi_{vv}$. The simulated reflection amplitude and phase with polarization along u- and v-axis are shown in Fig. 4. From Fig. 4(a), it can be seen that the reflection amplitudes in u- and v-axes directions are close to unity while the phase difference is about $-\pi(\pi)$ throughout the wavelength range where the linear polarization conversion occurs, which will lead to a 90° polarization rotation when EM wave is incident with polarization along the x- or y-axes of the MM.

4. CONCLUSIONS

In conclusion, we have proposed a simple structured MM to provide double-broadband polarization conversion. The proposed MM can convert a linearly polarized wave to its cross-polarized wave and circularly polarized wave to its co-polarized wave with high polarization conversion ratio larger than 0.9

in two different bands. The polarization conversion mechanism can be interpreted through analyzing the amplitude and phase variation between the incident and reflected waves. Experimental results coincide with the numerical simulations. The proposed simple geometrical MM-based polarizer is quite useful in designing novel high performance polarimetric devices for potential applications.

ACKNOWLEDGMENT

This work was supported by the Fundamental Research Funds for the Central Universities (No. CCNU16A0216).

REFERENCES

1. Veselago, V. G., "The electrodynamics of substances with simultaneously negative values of ε and μ," *Sov. Phys. Usp.*, Vol. 10, No. 4, 509–514, 1968.
2. Smith, D. R., J. B. Pendry, and M. C. K. Wiltshire, "Metamaterials and negative refractive index," *Science*, Vol. 305, No. 5685, 788–792, 2004.
3. Hoffman, A. J., L. Alekseyev, S. S. Howard, K. J. Franz, D. Wasserman, V. A. Podolskiy, E. E. Narimanov, D. L. Sivco, and C. Gmachl, "Negative refraction in semiconductor metamaterials," *Nat. Mater.*, Vol. 6, No. 12, 946–950, 2007.
4. Zhang, B., "Electrodynamics of transformation-based invisibility cloaking," *Light: Sci. Appl.*, Vol. 1, No. 10, e32, 2012.
5. Schurig, D., J. J. Mock, B. J. Justice, S. A. Cummer, J. B. Pendry, A. F. Starr, and D. R. Smith, "Metamaterial electromagnetic cloak at microwave frequencies," *Science*, Vol. 314, No. 5801, 977–980, 2006.
6. He, X. J., L. Wang, J. M. Wang, X. H. Tian, J. X. Jiang, and Z. X. Geng, "Electromagnetically induced transparency inplanar complementary metamaterial for refractive index sensing applications," *J. Phys. D: Appl. Phys.*, Vol. 46, No. 36, 510–516, 2013.
7. Wu, C., A. B. Khanikaev, R. Adato, N. Arju, A. A. Yanik, H. Altug, and G. Shvets, "Fano-resonant asymmetric metamaterials for ultra sensitive spectroscopy and identification of molecular monolayers," *Nat. Mater.*, Vol. 11, No. 1, 69–75, 2012.
8. Cheng, Y., C. Wu, Z. Z. Cheng, and R. Z. Gong, "Ultra-compact multi-band chiral metamaterial circular polarizer based on triple twisted split-ring resonator," *Progress In Electromagnetics Research*, Vol. 155, 105–113, 2016.
9. Cheng, Y. Z., W. Withayachumnankul, A. Upadhyay, D. Headland, Y. Nie, R. Z. Gong, M. Bhaskaran, S. Sriram, and D. Abbott, "Ultra broadband reflective polarization convertor for terahertz waves," *Appl. Phys. Lett.*, Vol. 105, No. 18, 181111–4, 2014.
10. Dincer, A. F., M. Karaaslan, E. Unal, O. Akgol, and C. Sabah, "Chiral metamaterial structures with strong optical activity and their applications," *Optical Engineering*, Vol. 53, No. 10, 107101–107108, 2014.
11. Zhang, L., P. Zhou, H. Chen, H. Lu, J. Xie, and L. Deng, "Adjustable wideband reflective converter based on cut-wire metasurface," *J. Opt.*, Vol. 17, No. 10, 105105, 2015.
12. Xie, L., H.-L. Yang, X. Huang, and Z. Li, "Multi-band circular polarization using archimedean spiral structure chiral metamaterial with zero and negative refractive index," *Progress In Electromagnetics Research*, Vol. 141, 645–657, 2013.
13. Yang, Y., W. Wang, P. Moitra, I. Kravchenko, D. P. Briggs, and J. Valentine, "Dielectric meta-reflect array for broadband linear polarization conversion and optical vortex generation," *Nano. Lett.*, Vol. 14, No. 3, 1394–1399, 2014.
14. Chen, H. T., W. J. Padilla, M. J. Cich, A. K. Azad, R. D. Averitt, and A. J. Taylor, "A metamaterial solid-state terahertz phase modulator," *Nat. Photon.*, Vol. 3, No. 3, 148–151, 2009.
15. Hsieh, C. F., R. P. Pan, T. T. Tang, H. L. Chen, and C. L. Pan, "Voltage-controlled liquid-crystal terahertz phase shifter and quarter-wave plate," *Opt. Lett.*, Vol. 31, No. 8, 1112–1114, 2006.

16. Rogacheva, A. V., V. A. Fedotov, A. S. Schwanecke, and N. I. Zheludev, "Giant gyrotropy due to electromagnetic-field coupling in a bilayered chiral structure," *Phys. Rev. Lett.*, Vol. 97, No. 17, 177401, 2006.
17. Ye, Y., X. Li, F. Zhuang, and S. W. Chang, "Homogeneous circular polarizers using a bilayered chiral metamaterial," *Appl. Phys. Lett.*, Vol. 99, No. 3, 031111-3, 2011.
18. Cao, Y., Y. Xie, Z. Geng, J. Liu, Q. Kan, and H. Chen, "Polarization-sensitive coupling and transmission dip shift in asymmetric metamaterials," *J. Phys. Chem. C*, Vol. 119, No. 11, 6204–6210, 2015.
19. Jiang, S. C., X. Xiong, Y. S. Hu, Y. H. Hu, G. B. Ma, R. W. Peng, C. Sun, and M. Wang, "Controlling the polarization state of light with a dispersion-free metastructure," *Phys. Rev. X*, Vol. 4, No. 2, 021026, 2014.
20. Li, Z., S. Chen, C. Tang, W. Liu, H. Cheng, Z. Liu, J. Li, P. Yu, B. Xie, Z. Liu, J. Li, and J. Tian, "Broadband diodelike asymmetric transmission of linearly polarized light in ultrathin hybrid metamaterial," *Appl. Phys. Lett.*, Vol. 105, No. 20, 201103-5, 2014.
21. Song, K., Y. Liu, C. Luo, and X. Zhao, "High-efficiency broadband and multiband cross-polarization conversion using chiral metamaterial," *J. Phys. D: Appl. Phys.*, Vol. 47, No. 50, 505104, 2014.
22. Tamayama, Y., K. Yasui, T. Nakanishi, and M. Kitano, "A linear-to-circular polarization converter with half transmission and half reflection using a single-layered metamaterial," *Appl. Phys. Lett.*, Vol. 105, No. 2, 021110-4, 2014.
23. Wu, J., B. Ng, H. Liang, M. Breese, M. Hong, S. A. Maier, H. O. Moser, and O. Hess, "Chiral metafoils for terahertz broadband high-contrast flexible circular polarizers," *Phys. Rev. Appl.*, Vol. 2, No. 1, 014005, 2014.
24. Liu, D. Y., M. H. Li, X. M. Zhai, L. F. Yao, and J. F. Dong, "Enhanced asymmetric transmission due to Fabry-Perot-Like cavity," *Opt. Express*, Vol. 22, No. 10, 11707–11712, 2014.
25. Mutlu, M. and E. Ozbay, "A transparent 90° polarization rotator by combining chirality and electromagnetic wave tunneling," *Appl. Phys. Lett.*, Vol. 100, No. 5, 051909-4, 2012.
26. Tremain, B., H. J. Rance, A. P. Hibbins, and J. R. Sambles, "Polarization conversion from a thin cavity array in the microwave regime," *Sci. Rep.*, Vol. 5, No. 9366, 2015.
27. Huang, S., J. Li, A. Zhang, J. Wang, and Z. Xu, "Broadband cross polarization converter using plasmon hybridizations in a ring/disk cavity," *Opt. Express*, Vol. 22, No. 17, 20973–20981, 2014.
28. Ma, H. F., G. Z. Wang, G. S. Kong, and T. J. Cui, "Broadband circular and linear polarization conversions realized by thin birefringent reflective metasurfaces," *Opt. Mater. Express*, Vol. 4, No. 8, 1717–1724, 2014.
29. Ding, F., Z. Wang, S. He, M. S. Vladimir, and V. K. Alexander, "Broadband high-efficiency half-wave plate a supercell-based plasmonic metasurface approach," *ACS Nano.*, Vol. 9, No. 4, 4111–4119, 2015.
30. Nanfang, Y., P. Genevet, M. A. Kats, F. Aieta, J. P. Tetienne, F. Capasso, and Z. Gaburro, "Light propagation with phase discontinuities: Generalized laws of reflection and refraction," *Science*, Vol. 334, No. 6054, 333–347, 2011.